Science of the Total Environment 955 (2024) 176840

Contents lists available at ScienceDirect

Science of the Total Environment

journal homepage: www.elsevier.com/locate/scitotenv

Assessing 7-year heat-stress exposures and adaptation strategies for children using a real-time monitoring network in Taiwan

Shih-Chun Candice Lung [a,b,c,*], Shu-Chuan Hu [a], Chun Hu Liu [a], Tzu-Yao Julia Wen [a], Wen-Cheng Vincent Wang [a,d]

[a] Research Center for Environmental Changes, Academia Sinica, Nangang, Taipei 115, Taiwan
[b] Department of Atmospheric Sciences, National Taiwan University, Taipei, Taiwan
[c] Institute of Environmental and Occupational Health Sciences, National Taiwan University, Taipei, Taiwan
[d] College of Applied Arts and Sciences, National Formosa University, Yunlin, Taiwan

HIGHLIGHTS

- This is the first heat-stress assessment for children, a vulnerable group.
- Hot-spot schools had >30 % of days from May to October with WBGTmax ≥36 °C.
- Effective adaptation strategies reduced % of dangerous days (WBGT ≥36 °C) to 0.
- Different from temperature, WBGT peaked before noontime in most schools.
- On-site monitoring can serve as a real-time heat-health alert tool.

GRAPHICAL ABSTRACT

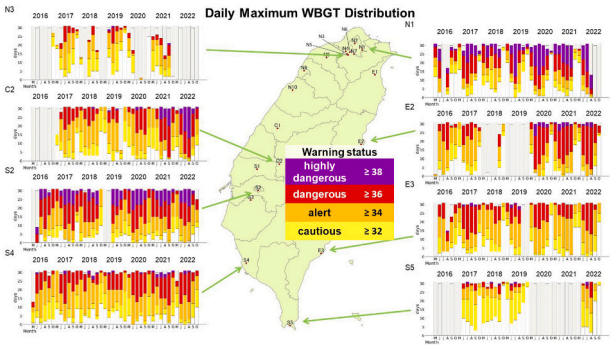

ARTICLE INFO

Editor: Pavlos Kassomenos

Keywords:
Heat and health
students' heat exposure
Children and heat
Health adaptation
Sustainable development goal 3

ABSTRACT

Wet-bulb globe temperature (WBGT) serves as a suitable heat-stress indicator not only for outdoor workers but also for the general public. However, studies on WBGT exposure among the general population are scarce. This research represents the first attempt to assess WBGT exposure of school-aged children. Utilizing a real-time monitoring network in Taiwan, WBGT exposure of school-aged children (7–15 years) were estimated during May to October from 2016 to 2022. Important determinants and spatiotemporal variability of WBGT levels were explored, with hot spots and peak hours of WBGT identified. Macro- and micro-scale adaptation strategies applicable at schools were also evaluated for their effectiveness in reducing heat stress for students. Results showed that the mean daily maximum WBGT (WBGTmax) was 33.1 ± 3.8 °C at 20 stations across Taiwan but could reach/exceed 36 °C (threshold of the dangerous category) at certain hot spots for 42.3–52.0 % of days between May and October. Local geographic features sometimes outweigh the latitude in explaining the spatial variations. Contrary to temperature, WBGT peaked during 10 am to noon rather than from noon to 1:59 pm in most schools, due to clouds blocking solar radiation in the afternoon. This finding has significant implications for scheduling outdoor physical classes/activities to reduce children's heat-health risks. Setting up on-site WBGT monitoring on surfaces that children mostly encounter at schools or utilizing data from nearby weather stations

* Corresponding author at: Research Center for Environmental Changes, Academia Sinica, No. 128, Sec. 2, Academia Rd, Nangang, Taipei 11529, Taiwan.
E-mail address: sclung@rcec.sinica.edu.tw (S.-C.C. Lung).

https://doi.org/10.1016/j.scitotenv.2024.176840
Received 5 July 2024; Received in revised form 4 October 2024; Accepted 8 October 2024
Available online 11 October 2024

could provide a near real-time heat-health warning. Moreover, providing shades outdoors, relocating outdoor classes indoors, and using air-conditioning would reduce WBGT by 2.1–5.8, 3.7–7.3, and 2.5–5.9 °C, respectively; and would significantly decrease the percentages of WBGT ≥34 °C, which is associated with increased heat-related emergency visits among children in Taiwan. The methodology applied serves as a useful reference for assessing WBGT exposure and adaptation strategies, providing the scientific foundation for heat-health adaptation measures.

1. Introduction

The entire earth experienced extreme heat in summer 2023. The Copernicus Climate Change Service, supported by the European Union, confirmed that summer 2023 was the hottest on record globally by a large margin, with an average temperature of 16.77 °C, 0.66 °C above average (C3S, 2023). Temperatures exceeded 50 °C on July 16th, 2023, in Death Valley in the U.S. and in Northwest China (C3S, 2023). Widespread and prolonged heat waves have occurred simultaneously in North America, Europe, and Asia not only in summer 2023 but also in summer 2022 (Lancet Planetary Health, 2022). In the U.S., stagnant heat domes had put more than 150 million people under heat warnings and advisories (NASA, 2022). Thousands of heat-related deaths occurred in Europe and Asia (WHO, 2022). The latest IPCC report indicated that hot extremes affect every inhabited region across the globe. Unless deep decarbonization occurs in the coming decades, global warming of 1.5 °C and 2 °C will be exceeded during the 21st century (IPCC, 2021). High casualty of hot extremes highlights the importance and urgency of effective heat adaptation strategies to reduce heat hazards, especially for the vulnerable populations (IPCC, 2022).

One of the vulnerable populations affected by hot extremes is children, as reviewed by Sheffield and Landrigan (2011), Vanos (2015), and Uibel et al. (2022). The report of the United Nations Children's Fund (UNICEF) stressed that around 500–600 million children are exposed to high frequency, duration, and severity of heatwaves (UNICEF, 2022). Children are physiologically susceptible to heat due to their smaller body surface-to-mass ratios; thus, they must divert more cardiac output to their skin to dissipate heat (Falk and Dotan, 2008); and they produce more heat per kilogram of weight than adults do (UNICEF, 2023). Children's thermoregulation functions are immature (Tsuzuki, 2023) and their cardiopulmonary systems are still developing (Hodges et al., 2018). In addition, children often spend more time outdoors than adults, especially during physical education at schools or outdoor leisure activities, and may thus be exposed longer to heat (USEPA, 2023). Most importantly, childhood health sets the trajectory for their adult health and productivity (Uibel et al., 2022); thus, the impacts of extreme heat on children's health may have lasting effects on their quality of life through adulthood. The reasons above underscore the importance of children-focused health adaptation strategies. Conducting heat exposure assessment for children serves as the initial step in understanding the status and determinants of their heat-stress exposure, laying the scientific foundation for potential adaptation strategies.

Selecting an appropriate indicator for heat stress is crucial for conducting such an assessment. Our previous heat-health assessment utilizing a population healthcare database in Taiwan demonstrated a correlation between increase in heat-related emergency visits and wet-bulb globe temperature (WBGT) (Cheng et al., 2019). For over 70 years, WBGT has been applied in occupational health to safeguard workers from heat stress, with a threshold of 32.2 °C indicating the onset of dangerous conditions signed by the black flag. WBGT considers four essential meteorological parameters of heat stress, namely, temperature, relative humidity (RH%), solar radiation (SR), and wind speed (WS) (Bernard, 2012). Prior research has shown association of WBGT with heat-related health impacts of both workers (Bröde et al., 2018; ISO, 2017; Spector and Sheffield, 2014; Yaglou and Minard, 1957) and of the general public (Kakamu et al., 2017; Lin et al., 2012; Lung et al., 2021). WBGT is viewed as the most suitable indicator to represent heat stress among all temperature-related indicators (ISO 7243, 1989). Since the purpose of heat adaptation strategy is to reduce health risks rather than enhancing thermal comfort, an indicator representing heat stress is more appropriate than other indictors representing human comfort or perception such as apparent temperature or Universal Thermal Climate Index (UTCI) (Coccolo et al., 2016; Höppe, 2002). However, few studies have monitored WBGT exposure of the general public. To make up for such deficiency, the current study conducted WBGT exposure assessment focusing on children, one of the vulnerable subpopulations.

Searching the Web of Science in September 2024, there are 158 publications with keywords of WBGT, worker, and exposure while only two with keywords of WBGT, children, and exposure. Within these two publications, one study assessed thermoregulation and fluid balance during exercise comparing sun-exposure and shaded conditions focused on only nine children (Santana et al., 1995) and the other was an epidemiological analysis using a population database without monitoring the WBGT exposure in children's living environment (Lung et al., 2021). In fact, no study has ever measured WBGT in children's living environment, as in the current study.

In Taiwan, the rise in temperature in urban areas was twice of the global increase (CWA, 2022). Despite a high air-conditioning prevalence (93 %, TNDC, 2018), heat-related health impacts were still observed when WBGT exceeded certain thresholds (Lin et al., 2012; Cheng et al., 2019; Lung et al., 2021). Cheng et al. (2019) found that children aged 0–14 had the highest relative risk (RR = 6.86, confidence interval (CI) = (1.49, 31.65)) in heat-related emergency visits when the daily maximum WBGT (WBGTmax) was ≥33 °C, compared with adults aged 15–64 (RR = 3.86, CI = (2.52, 5.91)) and the elderly (aged ≥65, RR = 5.50, CI = (2.50, 12.13)). Moreover, increase in heat-related hospital visits among children aged 0–14 was also observed at WBGTmax ≥32.5 °C (Lung et al., 2021). In Taipei metropolitan, the RR of the heat-related emergency visits among children aged 0–14 was 8.32 (1.96, 35.3) at WBGTmax ≥36 °C (Lung et al., 2023). Hence, there is an urgent need for WBGT exposure assessment for children to establish effective strategies for reducing their heat-related health impacts.

The present study focuses on assessing WBGT exposure among school-aged children (7–15 years old) during outdoor physical education classes or when playing in school fields during breaks. Specifically, WBGT levels during May to October from 2016 to 2022 were estimated using a real-time monitoring network. The important determinants of WBGT were explored and its spatiotemporal variability was evaluated to identify hot spots and peak hours of WBGT exposure across Taiwan. Scenarios with heat adaptation strategies were examined to evaluate their effectiveness. The lessons learned have implications for formulating heat adaptation strategies for children in other countries as well. Implementing adaptation strategies can reduce health risks to meet the United Nations Sustainable Development Goal 3 (SDG3), ensuring healthy living, and promoting well-being for populations at all ages (UN, 2018).

2. Methods

The following subsections describe the WBGT monitoring strategy, temporospatial assessment, and adaptation strategy evaluation.

2.1. Monitoring strategy

WBGT data were obtained using the equations derived by Liljegren et al. (2008) with meteorological observations of the Central Weather Administration (CWA), Taiwan. These equations are recognized by the Occupational Safety and Health Administration (OSHA), USA, as a valid method for estimating WBGT when direct measurements with traditional WBGT monitors are unavailable (OSHA, 2017). Liljegren equations were validated with WBGT measurements at seven locations in the US spanning a wide range of environmental conditions (Liljegren et al., 2008). The root mean square difference between the model-calculated WBGT and the measurements was less than 1 °C at these locations. Since these equations are derived based on thermodynamic principles of heat and mass transfer, they can be applied to any locations, unlike other site-specific empirical equations (Lemke and Kjellstrom, 2012). The inputs required for the WBGT equations include temperature, RH%, SR, and WS, as well as latitude and longitude of the monitoring sites.

Meteorological observations from 2016 to 2022 were collected from solar-powered HOBO weather stations (HOBO, RX3003 & RX3004, Onset, Bourne, MA, USA) set up by our team. These observations were wirelessly transmitted to the cloud storage maintained by our group for calculating WBGT with a lead time of 10–15 min. Only WBGT measurements taken during the hot seasons, defined as May to October according to Taiwan's climate (Chou et al., 2023), were utilized in this study. Based on the Taiwan's climatology, weather conditions from May to October are affected by the Pacific high pressure system while those in the other months are affected by the Mongolian high pressure system.

In addition to their wireless transmission capability, these HOBO stations are movable and significantly less expensive than a standard CWA weather station. Since 2016, we have gradually established a WBGT monitoring network of 20 HOBO stations, covering the entire Taiwan with 10 stations in the north, 2 in the central region, 5 in the south, and 3 in the east. These stations were positioned inside or near elementary and middle schools (details listed in the Supplemental Material Table S1), allowing the WBGT data obtained to approximate the children's outdoor exposure in and around the school premises. Unlike standard CWA stations typically situated on grassland, these 20 HOBO stations, with the exception of one, were installed at 2 m above concrete surfaces to assess actual WBGT exposure of children on these surfaces. Most of these stations were installed at heights of three to five floors to avoid interfering with children's activities. The distance of these stations to the center of the school fields where children play outdoors are within 500 m, with only two exceptions, 630 m and 770 m (Table S1). All the measurements can be found in the data repository (https://pid.depositar.io/ark:37281/k5d432n86).

It should be noted that station N3, the only one situated on grassland, was set up within a CWA station for comparison. The HOBO sensors were installed at the same heights as the CWA monitors (Table S1). The correlation coefficients of hourly HOBO and CWA observations from October 2016 to August 2022 are 0.987, 0.887, 0.778, and 0.953 for temperature, RH%, WS, and SR, respectively. The less expensive HOBO anemometer (resolution, 0.5 m/s) is not as precise as the CWA monitors (resolution, 0.1 m/s), resulting in a weaker correlation for WS compared with other parameters. However, the correction for the calculated WBGT from HOBO sensors versus CWA monitors is 0.956, indicating that WBGT data from HOBO are suitable for research purposes.

2.2. WBGT temporospatial assessment

To calculate WBGT, one-minute meteorological observations were used, excluding rainy periods. Given the focus on exposure of school-aged children, only hourly means of WBGT between 8 am and 5 pm (during school hours) were analyzed. WBGTmax represents the maximum of these hourly WBGT means in one day. Many schools organize summer activities, leading children to spend time on school fields during summer breaks in July and August. In this study, WBGT was monitored during May to October from 2016 to 2022. However, when evaluating potential adaptation strategies intended for use by school principals, only WBGT data from May, June, September, and October were used.

Moreover, WBGT is classified into four categories according to the WBGT warning system established by the CWA (https://opendata.cwa.gov.tw/dataset/forecast/M-A0085-001) which is founded on heat-health epidemiological findings evaluated in Taiwan. Significant increases in heat-related emergency visits among the general population of Taiwan population, residents in Taipei, and children in Taipei were found when WBGTmax was $\geq$32 °C, 34 °C, and 36 °C, respectively (Cheng et al., 2019; Lung et al., 2021; Lung et al., 2023). As a result, the four WBGT categories are defined as cautious, alert, dangerous, and highly dangerous when the WBGTmax was $\geq$32 °C and $<$ 34 °C, $\geq$ 34 °C and $<$ 36 °C, $\geq$ 36 °C and $<$ 38 °C, and $\geq$ 38 °C, respectively. These categories are color-coded as yellow, orange, red, and purple, respectively.

Furthermore, the hotspots within these 20 HOBO stations were assessed, and the determinants of WBGT were examined. Monthly trends for both WBGT and daily maximum temperature (Tmax) of these 20 stations over the seven-year period were analyzed to determine if they exhibited similar temporal distributions. Peaks during school hours (8 am to 5 pm) were identified for both WBGT and temperature to facilitate scheduling physical education classes at optimal times. Paired-*t*-tests were conducted to compare meteorological parameters and WBGT between the two hours before (10 am to noon, before-noon period) and after noon (noon-1:59 pm, afternoon period) on school days, with open source Python 3.11 (https://www.python.org/) and Scipy 1.11.3 (https://scipy.org/).

2.3. Adaptation strategy evaluation

Finally, both macro-scale (central government) and micro-scale (local school) health adaptation strategies were proposed and evaluated. The macro-scale adaptation strategy proposed is to use observations from standard CWA stations across Taiwan as a proxy for children's WBGT exposure. WBGT levels obtained by our monitoring network were compared with those observed at the nearest standard CWA station using paired-t-tests. Discrepancies are expected due to differences in installation location, with CWA stations situated on grassland, rather than concrete surfaces, as well as variations in distances between CWA stations and schools. If the WBGT difference falls within an acceptable range (e.g., 1–2 °C), the measurements from the nearest CWA station could be transmitted to local schools to serve as near real-time warnings.

Three micro-scale adaptation strategies were evaluated in terms of their expected reduction in WBGT. To assess the outdoor strategy of providing shades for outdoor activities, outdoor WBGT was calculated by setting SR as zero, while keeping the other meteorological parameters the same as the observations at the respective school. As for the strategy of relocating classes indoors and utilizing fans with open windows to reduce exposure, indoor WBGT was calculated using the indoor WBGT formula, with SR set as zero, RH% and WS as observed, and temperature reduced by 1.5 °C from the outdoor observations obtained at the respective school. To evaluate the indoor strategy of using air conditioning in classrooms, indoor WBGT was calculated and compared with that in the aforementioned open-window scenario. The indoor meteorological parameters were temperature of 27 °C, no solar radiation, WS of 0.3 m/s, and RH% reduced by 15 % from the observed levels.

All the above indoor settings were based on previous measurements conducted in Taiwan in both indoor and outdoor environments of 500 households under the open-window and air-conditioning conditions, except for temperature in the air-conditioning scenario. Along with its policy of installing air conditioners at all schools to reduce the impact of infiltrating hot outdoor air on classroom environments, the government of Taiwan recommended setting air-conditioning temperature between 26 °C and 28 °C for human comfort without consuming too much

energy. Thus, 27 °C was chosen for our scenario analysis.

3. Results

The following subsections provide our findings on WBGT temporospatial variations, determinants of WBGT hot spots and peak hours, and the assessment of potential health adaptation strategies.

3.1. WBGT temporospatial variations

Table 1 shows the mean, standard deviation (SD), maximum, sample size, and percentage of hourly WBGT ≥36 °C at 20 HOBO stations between 8 am and 5 pm from 2016 to 2022. The overall WBGT mean for the entire monitoring period was 30.8 ± 3.7 °C. The highest annual mean of hourly WBGT at all stations, 31.5 ± 3.3 °C, occurred in 2021; while the maximum hourly WBGT recorded during the entire monitoring period was 42.2 °C, observed at N2 in 2020. The overall mean of hourly WBGT for each station throughout the entire monitoring period ranged from 29.5 ± 3.6 °C (N8) to 32.6 ± 3.3 °C (S2).

To assess heat exposure, it is more important to evaluate the distributions of the daily WBGTmax for understanding the high heat-stress levels. Table 2 summarizes the WBGTmax at 20 HOBO stations from 2016 to 2022. The overall mean of WBGTmax for the entire monitoring period was 33.1 ± 3.8 °C. The highest annual mean of WBGTmax at all stations, 33.8 ± 3.4 °C, occurred in 2021. The overall means of WBGTmax for each station throughout the entire monitoring period ranged from 31.2 ± 3.9 °C (N8) to 35.5 ± 2.8 °C (S2). While most stations had an overall mean of WBGTmax in the cautious range (between 32 °C and 34 °C), the means of N3, N8, and N9 were below the cautious range (< 32 °C) and those of C2, S2, S4, and E3 were in the alert range (between 34 °C and 36 °C). The two highest overall means in % of WBGTmax ≥36 °C among the 20 stations during the seven-year period were 48.5 % (S2) and 41.9 % (N1). The bottom rows of Table 2 show the overall summary of temperature measurements for comparison. Interestingly, the top two stations with the highest % of Tmax ≥36 °C were N6 and N7, differing from those identified using WBGT.

Factors contributing to variations in WBGTmax within the four regions of Taiwan were examined using data collected from 2019 to 2021, which has the most complete monitoring with only one station missing (Table 2). Among the northern stations, N1 – N7 are situated within the Taipei basin, characterized by more pronounced heat accumulation than the open field areas. Consequently, WBGTmax means in N1 – N7 are generally higher than those in N8–N10, sometimes even exceeding those in the central and southern stations. There are also spatial variations among N1 – N7, possibly influenced by local geographic features. N1 (33.7 ± 4.9 °C) and N4 (33.9 ± 4.3 °C) have the top two highest mean WBGTmax among all northern stations. Of note is that they are not located in the city center where the urban heat island effect is most pronounced (Wu and Lung, 2016). N1 is situated in an area surrounded by mountains on three sides, and N4 is in an area surrounded by mountains on one side. According to the RH%, WS, and SR data (Table S2), the relatively lower WS at these two stations resulted in higher WBGT compared with the rest of the northern stations. In central Taiwan, C2 is situated in the Central Mountain region. Surrounded by mountains, C2 has higher RH% and lower WS, resulting in consistently higher WBGT than C1, despite its temperatures being constantly lower than those at C1 (Table S2). In the south, S2, exhibiting the highest temperatures among the stations (Table S2), has the highest WBGT, the highest mean WBGTmax from 2016 to 2021 and the second highest in 2022, with an annual mean WBGTmax consistently ≥35 °C. While S2 is not the southernmost station of the monitoring network, its location in an area where the Tropic of Cancer passes may account for its frequently higher WBGT levels compared with other stations. In the east, E2 and E3 consistently exhibit higher WBGT levels than E1, the northernmost station in the eastern region. The present findings highlight significant spatial variations among stations within the same region. Latitude and local geographic features, such as being surrounded by mountains, emerge as crucial determinants influencing WBGTmax levels.

The percentages of WBGTmax in the dangerous category show severe WBGT exposure in the outdoor environments of these schools (Table 2). In certain years, more than half of the stations recorded WBGTmax ≥36 °C for more than 10 % of days. N1 and N4 experienced more than 30 % of days with WBGTmax ≥36 °C every year, while S2 had over 40 % of days with WBGTmax ≥36 °C in three years and over 50 % in the other four years, showing significant heat stress in these areas. Most stations recorded the highest percentage of WBGTmax ≥36 °C in 2021 or 2022. It is essential to understand the temporospatial distribution of the WBGTmax above health-concerned thresholds since these high WBGT levels could induce heat-related illness.

Fig. 1(a) displays the monthly variations in WBGTmax at the 20 stations over the seven-year period. The maximum and 95th percentile of WBGTmax are scattered across June, July, August, and September in different years, highlighting the unpredictable nature of extreme events. The percentage of WBGTmax ≥36 °C is notably higher between 2020 and 2022 compared with earlier years, echoing the global trend of increased frequency of extreme heat events during this period.

The monthly variations in Tmax are also depicted in Fig. 1(b) for comparison. Although the monthly distribution patterns of WBGT and temperature appear similar, some differences exist. Notably, the highest 95th percentiles of both WBGTmax and Tmax for the same year do not consistently occur in the same month. For instance, in 2017, the highest 95th percentile of WBGTmax occurred in July, whereas that of Tmax was in August. Furthermore, while July and August typically have the top two highest WBGTmax medians among these six months, except in 2021, the highest Tmax medians among these six months all occurred in July over the seven years. The highest 95th percentile of WBGTmax over these seven years occurred in August 2020, whereas the highest 95th percentile of Tmax occurred in July 2022. These two graphs demonstrate different hottest months identified using different indicators.

Table 3 presents a comparison of hourly WBGT between school days (May, June, September, and October) and summer breaks (July and August). The WBGT means for all stations are consistently higher during summer breaks (range, 31.5–33.6 °C) than on school days (range, 28.3–32.0 °C). However, eight stations exhibit a higher hourly WBGTmax on school days than during summer breaks. These stations are distributed across the northern (N8 and N10), central (C1), southern (S3, S4, and S5), and eastern (E2 and E3) regions. These findings reveal that children playing in school fields experience high heat levels both during school days and summer breaks, with peak exposures occurring in either period. However, at the same station, the percentage of hourly WBGT ≥36 °C is consistently higher during summer breaks than on school days. The top three stations with the highest percentages both on school days and during summer breaks are S2, N1, and N4.

3.2. Determinants of WBGT hot spots and peak hours

Fig. 2 shows the numbers of days with daily WBGTmax falling into different warning categories during May to October from 2016 to 2022 at eight selected stations, including the top one station (hot spot) in each region with the highest percentage of WBGTmax ≥36 °C, namely N1, C2, S2, and E2. The other four stations are N3 situated within a CWA station and S4, S5, and E3, the three southernmost stations. At most of these eight stations, the numbers of purple days (highly dangerous category) between 2020 and 2022 are higher than those in earlier years.

Significant spatial variability is evident every year, therefore, factors contributing to the spatial variations were further evaluated. N1 and S2 had more purple days than other stations (Fig. 2). In 2020, 2021, and 2022, N1 had 51, 47, and 32 purple days, and S2 had 37, 32, and 27 purple days, respectively. Different geographical surroundings and monitoring conditions contribute to variations in RH%, WS, and SR (Table S1) and, consequently, WBGT levels. For instance, both N3 and N1 are in the same basin; N3 is situated at 1.7 km from the surrounding

Table 1
Means, standard deviations (SD), maximum (Max), sample size in terms of hours measured, and the percentage ≥ 36 °C (threshold of the dangerous category) of hourly wet-bulb globe temperature (WBGT) of the 20 stations from 8 am to 5 pm during May to October in 2016–2022; N, C, S, and E denote northern, central, southern, and eastern region, respectively.

Year	Station	N1	N2	N3	N4	N5	N6	N7	N8	N9	N10	C1	C2	S1	S2	S3	S4	S5	E1	E2	E3	All
2016	Mean	30.5	–[a]	27.7	–	–	–	–	–	–	30.4	30.4	–	–	33.1	–	32.3	–	–	31.5	32.0	31.3
	SD	4.0	–	3.2	–	–	–	–	–	–	3.1	2.4	–	–	2.9	–	2.6	–	–	2.9	2.8	3.2
	Max	38.9	–	34.9	–	–	–	–	–	–	41.1	36.3	–	–	40.1	–	38.7	–	–	37.9	38.3	41.1
	Hour	1113	–	227	–	–	–	–	–	–	1723	1234	–	–	1149	–	1452	–	–	1381	1144	–
	% ≥ 36 °C	10.3	–	0.0	–	–	–	–	–	–	4.3	0.1	–	–	15.5	–	5.1	–	–	3.7	4.1	5.7
2017	Mean	30.9	–	30.0	–	–	–	–	30.3	30.1	30.3	29.7	31.3	31.1	32.8	25.3	32.1	31.0	30.0	30.9	31.7	30.9
	SD	4.4	–	3.8	–	–	–	–	2.8	3.3	3.4	3.1	3.1	3.1	3.2	2.6	2.8	2.6	3.6	3.7	3.6	3.5
	Max	41.1	–	37.8	–	–	–	–	37.2	36.9	39.3	35.3	37.5	38.8	40.4	32.3	38.6	38.1	36.3	37.7	38.5	41.1
	Hour	1544	–	1420	–	–	–	–	1420	1534	1702	912	1434	1529	1633	100	1723	1368	1485	1657	1677	–
	% ≥ 36 °C	12.2	–	2.0	–	–	–	–	0.6	0.1	3.8	0.0	4.1	3.0	14.5	0.0	5.6	1.5	0.2	2.9	8.8	4.5
2018	Mean	30.2	–	30.4	31.2	–	30.0	29.9	29.0	29.8	29.4	29.4	30.9	30.6	32.0	30.7	31.7	30.4	29.6	28.1	31.0	30.3
	SD	4.3	–	3.1	4.3	–	4.0	4.2	3.7	3.4	3.3	2.7	3.1	3.0	3.4	3.2	2.7	2.9	3.6	4.3	3.4	3.6
	Max	41.3	–	37.1	40.3	–	38.1	38.9	37.6	36.5	38.1	35.6	38.5	37.9	40.2	38.4	38.4	38.6	36.9	37.7	37.7	41.3
	Hour	1613	–	721	1696	–	1663	1633	1683	1656	1735	1703	1622	1723	1669	1675	1616	1592	1671	486	1680	–
	% ≥ 36 °C	7.7	–	1.7	12.6	–	2.6	4.8	0.5	0.2	1.1	0.0	3.3	2.2	11.4	3.1	2.8	1.8	0.4	2.7	1.8	3.4
2019	Mean	30.3	30.0	29.7	30.7	27.0	29.9	29.7	28.8	29.5	30.0	29.3	30.5	30.4	32.2	30.3	31.7	29.8	30.4	–	31.5	30.1
	SD	4.5	3.8	3.9	4.4	3.8	4.3	4.2	3.9	3.6	3.0	2.9	3.2	3.1	3.4	3.3	2.9	2.7	3.6	–	3.5	3.7
	Max	40.8	37.5	39.1	40.3	36.6	38.9	39.2	38.5	36.9	38.9	35.9	38.7	38.5	41.0	38.6	38.2	39.3	39.7	–	38.7	41.0
	Hour	1530	1493	1339	1605	546	1595	1573	1636	1680	1060	1663	1358	1687	1085	1700	1605	1607	1059	–	1109	–
	% ≥ 36 °C	9.6	2.2	2.2	10.0	0.2	3.4	3.5	0.5	0.2	2.3	0.0	2.5	1.7	13.9	3.9	5.2	1.4	1.9	–	6.7	3.7
2020	Mean	31.4	30.0	27.7	31.4	30.1	30.6	30.5	29.5	30.0	28.0	30.0	31.3	31.1	32.8	31.0	32.4	–	30.0	31.5	31.5	30.8
	SD	4.5	4.5	4.1	4.2	3.9	4.2	4.2	3.6	3.2	3.5	2.6	3.1	2.8	3.3	3.1	2.7	–	3.7	4.2	3.4	3.8
	Max	41.1	42.2	37.2	40.3	38.4	39.5	39.1	38.0	37.4	36.8	35.8	38.9	38.8	41.3	39.1	38.3	–	37.5	39.5	38.0	42.2
	Hour	1521	1262	583	1644	1622	1637	1607	1682	1731	593	1716	1680	1716	1671	1677	1683	–	1591	1707	1728	–
	% ≥ 36 °C	17.9	8.1	0.9	10.3	1.2	4.9	5.9	1.4	0.2	0.7	0.0	4.3	2.2	15.9	3.4	5.8	–	1.1	14.1	4.3	5.6
2021	Mean	31.7	31.0	31.2	32.9	30.9	31.3	31.4	30.1	30.9	30.4	31.4	32.3	31.4	32.9	31.0	32.7	–	30.7	32.0	31.8	31.5
	SD	4.0	3.6	2.8	3.0	3.5	3.6	3.7	3.1	2.9	2.8	3.2	3.3	2.7	3.1	3.2	2.7	–	3.2	3.6	2.9	3.3
	Max	41.4	38.5	38.6	40.3	38.4	40.1	39.8	36.9	36.8	37.7	41.4	40.4	39.0	40.0	38.8	38.6	–	36.9	38.7	37.8	41.4
	Hour	1589	1673	865	1506	1596	1635	1598	1680	1704	1686	1662	1598	1680	1623	1823	1576	–	1630	1713	1718	–
	% ≥ 36 °C	13.8	3.9	2.9	15.4	3.6	5.7	7.6	0.6	0.4	1.7	8.5	15.3	3.5	15.7	5.0	9.6	–	0.5	11.7	2.9	6.7
2022	Mean	31.9	–	–	–	30.0	30.5	30.7	29.2	29.8	29.5	31.2	32.5	30.9	32.5	30.6	32.0	31.0	30.1	31.3	31.4	30.8
	SD	4.6	–	–	–	4.5	4.8	4.8	4.1	3.7	3.5	3.6	3.7	3.3	3.4	4.0	2.9	2.9	3.8	4.2	3.5	4.0
	Max	40.7	–	–	–	38.7	38.8	39.9	38.3	36.8	37.3	39.9	40.1	39.5	40.5	40.6	38.5	38.1	36.7	38.8	38.0	40.7
	Hour	866	–	–	–	1524	1543	1487	1604	1654	1668	1672	1615	1697	1552	1733	1627	1403	1531	1639	1733	–
	% ≥ 36 °C	20.9	–	–	–	3.8	9.8	13.0	0.7	0.5	1.6	6.6	17.7	4.0	13.7	6.3	6.9	1.9	0.2	10.8	4.7	6.9
Overall	Mean	30.9	30.3	29.8	31.5	30.0	30.5	30.4	29.5	30.0	29.9	30.2	31.5	30.9	32.6	30.6	32.1	30.5	30.1	31.3	31.5	30.8
	SD	4.4	4.0	3.8	4.1	4.1	4.2	4.3	3.6	3.4	3.3	3.1	3.3	3.0	3.3	3.4	2.8	2.8	3.6	3.9	3.4	3.7
	Max	41.4	42.2	39.1	40.3	38.7	40.1	39.9	38.5	37.4	41.1	41.4	40.4	39.5	41.3	40.6	38.7	39.3	39.7	39.5	38.7	42.2
	% ≥ 36 °C	12.8	4.5	1.9	12.0	2.6	5.3	6.9	0.7	0.3	2.4	2.4	8.0	2.8	14.3	4.3	5.9	1.6	0.6	8.5	4.7	5.2

[a] Monitoring was not conducted.

Table 2
Means, standard deviations (SD), maximum (Max), sample size in terms of days measured, and the percentage ≥ 36 °C (threshold of the dangerous category) of daily maximum WBGT (WBGTmax) of the 20 stations from 8 am to 5 pm during May to October in 2016–2022; N, C, S, and E denote northern, central, southern, and eastern region, respectively. The bottom rows summarize daily maximum temperatures (Tmax) in 2016–2022.

Year	Station	N1	N2	N3	N4	N5	N6	N7	N8	N9	N10	C1	C2	S1	S2	S3	S4	S5	E1	E2	E3	All
2016	Mean	33.3	–[a]	29.3	–	–	–	–	–	–	33.0	32.4	–	–	35.6	–	34.4	–	–	34.1	34.2	33.7
	SD	4.4	–	3.8	–	–	–	–	–	–	3.6	2.2	–	–	2.6	–	2.4	–	–	2.5	2.5	3.2
	Max	38.9	–	34.9	–	–	–	–	–	–	41.1	36.3	–	–	40.1	–	38.7	–	–	37.9	38.3	41.1
	Day	133	–	27	–	–	–	–	–	–	183	131	–	–	131	–	163	–	–	151	129	–
	% ≥ 36 °C	36.8	–	0.0	–	–	–	–	–	–	23.5	0.8	–	–	55.0	–	24.5	–	–	21.9	23.3	25.6
2017	Mean	33.5	–	31.9	–	–	–	–	31.9	31.5	32.7	31.5	34.0	33.3	35.4	28.2	34.6	32.5	32.1	33.3	34.4	33.1
	SD	4.8	–	4.1	–	–	–	–	3.0	3.3	3.8	2.9	2.6	3.0	2.9	2.7	2.3	2.5	3.4	3.4	3.0	3.5
	Max	41.1	–	37.8	–	–	–	–	37.2	36.9	39.3	35.3	37.5	38.8	40.4	32.3	38.6	38.1	36.3	37.7	38.5	41.1
	Day	177	–	162	–	–	–	–	154	164	180	95	166	167	183	10	183	151	167	179	182	–
	% ≥ 36 °C	42.9	–	12.3	–	–	–	–	4.5	1.2	23.3	0.0	24.1	15.0	51.9	0.0	30.6	7.3	1.8	17.9	40.7	20.8
2018	Mean	33.0	–	32.7	33.7	–	32.4	32.4	30.8	31.4	31.6	31.2	34.0	33.0	35.1	33.4	34.1	32.0	32.0	31.3	33.4	32.7
	SD	4.9	–	3.4	4.5	–	4.2	4.5	4.0	3.5	3.5	2.5	2.3	2.7	2.9	3.0	2.5	2.9	3.6	4.1	2.9	3.7
	Max	41.3	–	37.1	40.3	–	38.1	38.9	37.6	36.5	38.1	35.6	38.5	37.9	40.2	38.4	38.4	38.6	36.9	37.7	37.7	41.3
	Day	180	–	84	184	–	183	184	183	175	184	184	184	183	181	182	180	179	182	56	181	–
	% ≥ 36 °C	31.1	–	8.3	37.0	–	16.4	23.4	3.3	2.3	8.2	0.0	16.3	13.1	43.6	19.8	17.2	8.4	3.3	12.5	14.4	15.8
2019	Mean	32.7	32.1	31.8	32.9	28.9	31.9	31.8	30.5	31.0	31.6	31.0	33.6	32.7	35.5	33.2	34.1	31.4	32.7	–	34.0	32.3
	SD	5.2	3.6	4.0	4.7	3.9	4.6	4.6	4.2	3.6	3.6	2.7	2.7	2.8	2.7	3.0	2.5	2.7	3.8	–	3.4	3.9
	Max	40.8	37.5	39.1	40.3	36.6	38.9	39.2	38.5	36.9	38.9	35.9	38.7	38.5	41.0	38.6	38.2	39.3	39.7	–	38.7	41.0
	Day	183	168	152	183	61	184	183	182	183	121	184	158	184	123	184	181	183	122	–	121	–
	% ≥ 36 °C	33.3	13.1	11.2	31.1	1.6	19.0	18.6	3.3	1.6	10.7	0.0	13.9	9.8	42.3	18.5	23.8	4.9	11.5	–	28.1	15.6
2020	Mean	34.4	32.4	29.8	33.6	32.1	33.0	33.0	31.4	31.4	30.3	31.8	34.5	33.3	36.0	33.8	35.0	–	31.9	34.3	34.0	33.2
	SD	5.0	5.0	4.7	4.5	4.1	4.3	4.4	3.8	3.3	4.0	2.2	2.2	2.4	2.4	2.5	2.0	–	3.9	3.7	2.8	3.9
	Max	41.1	42.2	37.2	40.3	38.4	39.5	39.1	38.0	37.4	36.8	35.8	38.9	38.8	41.3	39.1	38.3	–	37.5	39.5	38.0	42.2
	Day	175	143	70	180	180	179	180	180	183	62	183	184	184	184	181	181	–	184	184	184	–
	% ≥ 36 °C	51.4	23.8	7.1	33.3	7.2	26.3	27.2	8.3	1.6	4.8	0.0	27.2	11.4	54.9	18.8	33.7	–	7.6	46.2	26.6	23.1
2021	Mean	34.7	33.3	33.4	35.5	33.0	33.6	33.9	32.0	32.5	32.3	33.7	35.2	33.5	35.5	33.6	34.9	–	32.9	35.0	34.2	33.8
	SD	4.4	3.7	2.8	2.8	3.8	3.9	4.1	3.4	3.0	3.1	3.3	2.9	2.5	2.8	2.9	2.5	–	3.1	2.9	2.2	3.4
	Max	41.4	38.5	38.6	40.3	38.4	40.1	39.8	36.9	36.8	37.7	41.4	40.4	39.0	40.0	38.8	38.6	–	36.9	38.7	37.8	41.4
	Day	180	183	112	168	183	183	182	179	181	180	182	182	182	183	184	180	–	183	184	182	–
	% ≥ 36 °C	48.3	24.0	16.1	50.0	21.9	26.2	33.5	5.0	3.3	12.8	28.0	44.5	17.0	50.8	24.5	40.0	–	4.4	49.5	17.0	27.4
2022	Mean	34.5	–	–	–	31.8	32.4	32.8	30.8	31.3	31.3	33.8	35.5	33.2	35.1	33.7	34.5	32.5	31.6	33.8	33.7	33.1
	SD	5.3	–	–	–	5.0	5.1	5.3	4.3	3.9	3.9	3.6	3.1	3.4	3.2	3.7	2.6	2.9	4.2	4.2	3.1	4.2
	Max	40.7	–	–	–	38.7	38.8	39.9	38.3	36.8	37.3	39.9	40.1	39.5	40.5	40.6	38.5	38.1	36.7	38.8	38.0	40.7
	Day	102	–	–	–	176	179	176	177	180	182	184	182	183	177	182	178	153	180	181	184	–
	% ≥ 36 °C	52.9	–	–	–	18.2	33.5	40.3	5.1	2.2	12.1	29.3	52.7	18.6	40.7	25.8	34.3	9.2	1.1	47.5	25.0	25.8
Overall	Mean	33.7	32.6	31.9	33.9	32.0	32.7	32.8	31.2	31.5	32.0	32.2	34.5	33.2	35.5	33.5	34.5	32.1	32.2	33.9	34.0	33.1
	SD	4.9	4.1	4.0	4.3	4.4	4.5	4.6	3.9	3.5	3.7	3.0	2.7	2.8	2.8	3.1	2.4	2.8	3.7	3.6	2.9	3.8
	Max	41.4	42.2	39.1	40.3	38.7	40.1	39.9	38.5	37.4	41.1	41.4	40.4	39.5	41.3	40.6	38.7	39.3	39.7	39.5	38.7	42.2
	% ≥ 36 °C	41.9	20.2	11.0	37.6	14.3	24.2	28.5	4.9	2.1	14.7	9.3	30.2	14.1	48.5	21.2	29.2	7.4	4.6	35.7	24.9	21.8
Tmax																						
Overall	Mean	32.5	32.3	32.2	33.0	32.0	32.8	32.5	31.4	31.4	31.4	32.7	32.2	32.5	33.4	32.9	32.7	30.7	30.6	30.8	31.5	32.1
	SD	4.4	3.7	4.1	4.0	4.3	4.3	4.5	3.6	3.1	2.9	2.7	2.5	2.6	2.4	2.6	2.0	2.2	3.3	2.5	2.3	3.3
	Max	40.5	38.0	39.8	39.2	39.5	40.0	40.1	38.4	36.9	39.1	40.0	37.9	37.7	38.1	37.5	37.3	35.2	37.1	35.9	40.0	40.5
	% ≥ 36 °C	21.5	11.7	12.5	21.4	11.8	24.1	22.4	2.2	1.1	0.8	7.4	1.5	2.4	7.5	4.9	1.0	0.0	0.3	0.0	0.5	7.2

[a] Monitoring was not conducted.

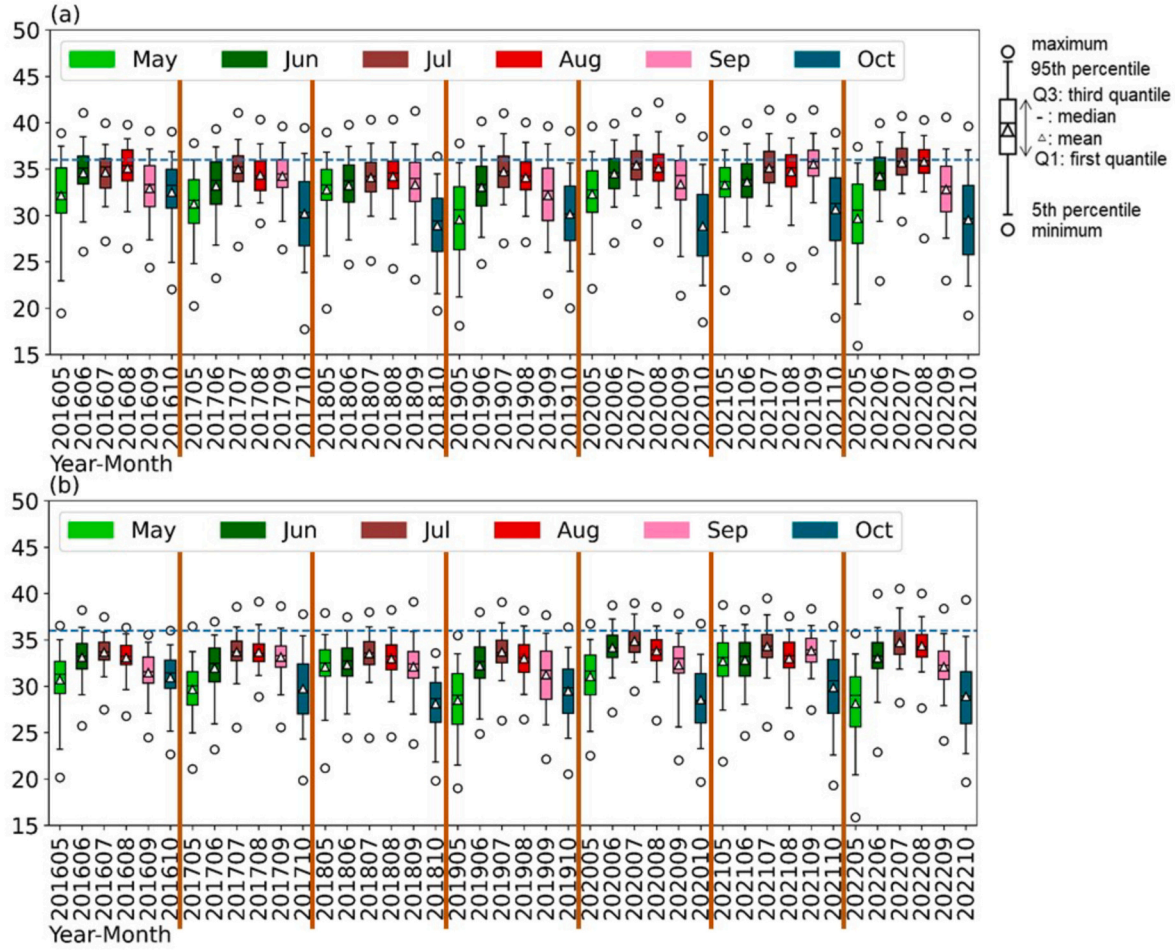

Fig. 1. Distribution of (a) daily WBGTmax and (b) daily Tmax of the 20 stations during May to October at 2016–2022. The dashed lines indicate 36 °C, the threshold of the dangerous category. Different color represents different months.

Table 3
Mean, standard deviation (SD), maximum (Max), sample size in terms of hours measured, and the percentage ≥ 36 °C (threshold of the dangerous category) of the hourly wet-bulb globe temperature (WBGT) of the 20 stations from 8 am to 5 pm on school days (May, June, September, and October) and during summer breaks (July and August) in 2016–2022.

	School day					Summer break				
Station	Mean	SD	Max	Sample size	% ≥ 36 °C	Mean	SD	Max	Sample size	% ≥ 36 °C
N1	29.8	4.5	41.3	6450	9.1	33.2	3.0	41.4	3326	19.8
N2	29.3	4.0	38.5	2997	2.1	32.6	2.7	42.2	1431	9.6
N3	28.7	3.9	38.8	3292	1.2	31.9	2.3	39.1	1863	3.3
N4	30.5	4.3	39.7	4236	7.9	33.6	2.7	40.3	2215	19.9
N5	28.7	4.1	37.8	3644	1.0	32.7	2.3	38.7	1644	6.1
N6	29.2	4.3	38.9	5298	2.3	33.0	2.5	40.1	2775	10.8
N7	29.2	4.4	38.6	5169	4.0	32.9	2.7	39.9	2729	12.4
N8	28.3	3.8	38.5	6230	0.5	31.5	2.1	38.3	3475	1.2
N9	28.9	3.6	36.8	6445	0.1	32.0	1.8	37.4	3514	0.6
N10	29.0	3.4	41.1	6712	1.6	31.5	2.2	39.8	3455	3.8
C1	29.5	3.2	41.4	6921	1.9	31.6	2.2	40.5	3641	3.4
C2	30.8	3.3	39.3	6193	4.7	32.8	3.0	40.4	3114	14.6
S1	30.3	3.1	38.8	6686	1.5	32.1	2.4	39.5	3346	5.2
S2	32.0	3.3	40.5	6674	10.5	33.6	2.9	41.3	3708	21.3
S3	30.3	3.5	40.6	5958	3.5	31.5	3.0	39.7	2750	6.1
S4	31.7	2.8	38.7	7632	4.4	32.9	2.5	38.6	3650	8.9
S5	29.9	2.9	39.3	3899	1.2	31.8	2.2	38.9	2071	2.5
E1	28.9	3.9	37.2	5455	0.2	32.0	2.1	39.7	3512	1.3
E2	30.2	4.0	39.5	5603	5.6	33.3	2.6	39.0	2980	14.1
E3	30.8	3.6	38.7	6909	3.5	32.9	2.4	38.5	3880	6.8
All	29.9	3.8	41.4	112,403	3.5	32.5	2.6	42.2	59,079	8.5

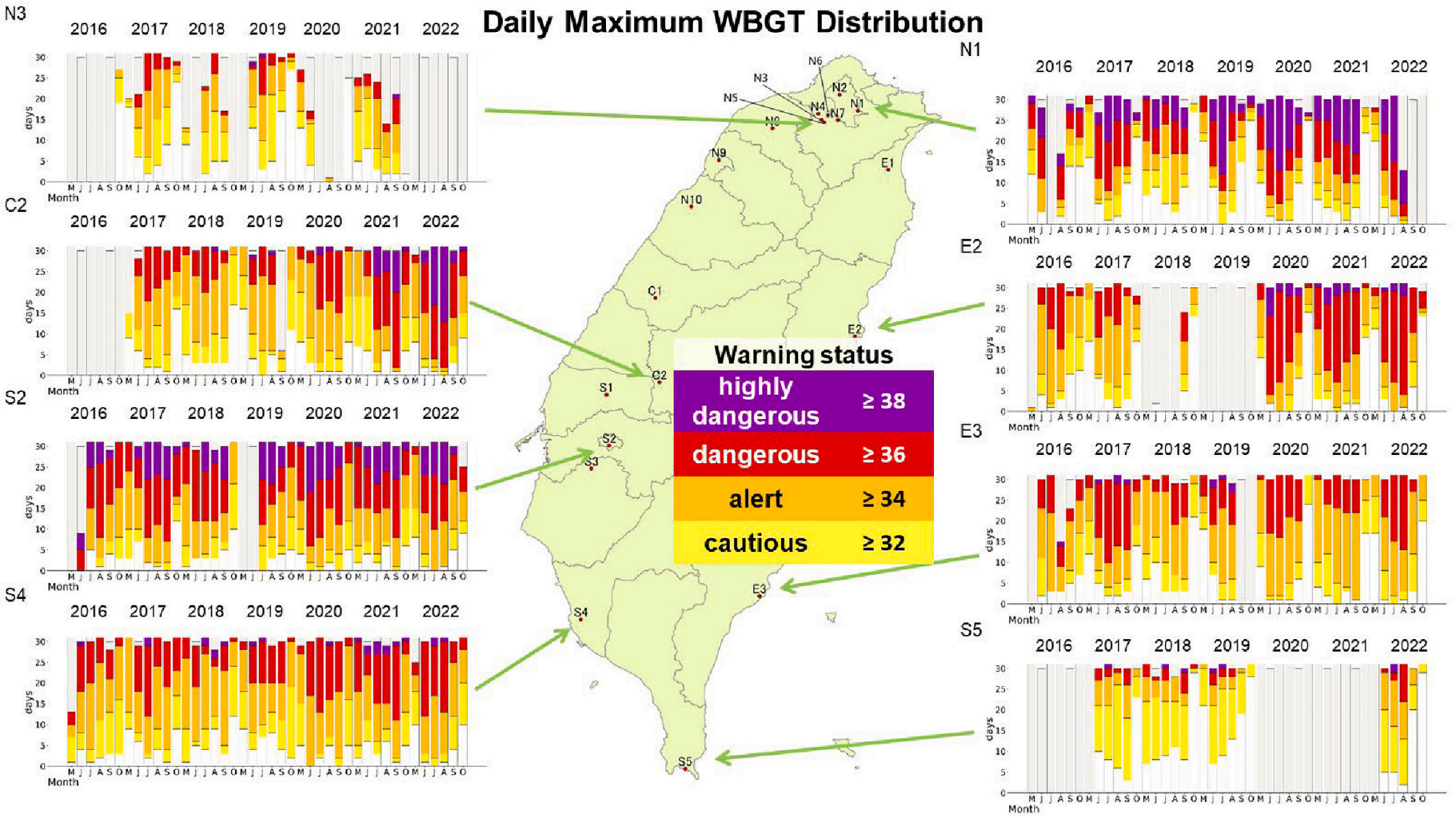

Fig. 2. Numbers of days with daily WBGTmax falling into different warning categories during May to October of 2016 to 2022 at eight selected stations across Taiwan. Yellow, orange, red, and purple indicate warning categories of cautious, alert, dangerous, and highly dangerous when the WBGTmax was ≥32 °C and < 34 °C, ≥ 34 °C and < 36 °C, ≥ 36 °C and < 38 °C, and ≥ 38 °C, respectively. White indicates WBGTmax below 32 °C and gray indicates missing data. Locations of all 20 stations are also shown in the graph.

mountains, where WBGT is monitored on grassland, while N1 is only 50–150 m away from mountains on three sides, where WBGT is monitored on a concrete surface. Heat accumulation in the basin and local geographic conditions cause N1 to have more days in the dangerous (red) and highly dangerous (purple) categories compared with all other stations located further south, except for S2. In 2019–2022, N1 experienced several months during which more than half of the month fell into the highly dangerous category. Specifically, at N1, July typically had more purple days than other months, except in 2021, when September had more purple days. In contrast, at S2, the months with the most purple days varied from June through September across different years, again highlighting temporal variability of hot extremes. Furthermore, S2 had more purple days than S4 and S5, despite both situated further south. Similarly, in the central and eastern regions, C2 and E2 consistently experienced more purple days than stations located further south, except for S2. However, the southernmost station, S5, positioned in an open area without mountains nearby, had significantly fewer days in red and purple categories due to the substantially higher WS in that area (Table S1). These cases demonstrate that local geographic features outweigh latitude in influencing WBGT levels.

The literature suggests that children are more vulnerable than adults, with those aged 0–14 in Taiwan experiencing increased heat-related emergencies at WBGTmax $\geq$33 °C (Lung et al., 2021). Hence, the days in orange, red, and purple categories in Fig. 2 indicate potential heat-health risks ($\geq$ 34 °C) for children attending these schools. It is evident that the majority of the monitoring days of these stations, except N3 and S5, are associated with potential heat-health risks for children.

In addition, contrary to temperature distribution, WBGT peaked in the before-noon period rather than in the afternoon period at almost all stations. Table 4 compares temperature, RH%, WS, and SR, and WBGT levels at the 20 stations between these two time periods. As can be seen, most stations have significantly lower temperature and WS but higher RH% and SR in the before-noon period than in the afternoon period, with $p < 0.0001$, resulting in significantly higher WBGT at most stations during the before-noon period, with $p < 0.0001$. Situated in the subtropical zone, Taiwan experiences frequent afternoon thunderstorms. Cloud formation typically begins around noon. The dense and towering cumulonimbus clouds with vertical dimensions from tens to thousands of meters would block SR resulting in reduced SR in the ground level in turn reduced WBGT levels during the afternoon period. This finding has significant implications for health adaptation strategies, such as scheduling outdoor physical classes.

3.3. Evaluation of potential health adaptation strategies

With the proposed macro-scale strategy, the differences in WBGT levels obtained at schools and the nearest CWA stations ranged between 1.1 and 4.7 °C, mostly within 3 °C except for N2, N4 and S2 (Table 5). All WBGT levels at schools are significantly higher, with $p < 0.0001$. Therefore, relying solely on WBGT levels observed at CWA stations would lead to underestimation of WBGT exposure experienced in school fields. The disparity in WBGT levels is not related to the distance between the school and the CWA station. For instance, N10, S1, and N8, situated the furthest from their respective CWA stations (17.6–32.3 km) have a WBGT difference within 2 °C; while N2, which has the largest WBGT difference, is only 5.4 km away from the nearest CWA station. The temperature difference (6 °C, Table S3) rather than distance accounts for the WBGT difference because the nearest CWA station, situated in the mountains, has a much lower temperature than the respective school.

Significant differences in temperature, RH%, WS, and SR at $p < 0.0001$ between schools and CWA stations were observed (Table S3), with lower temperature and RH% but higher WS and SR at most CWA stations. Differences in SR fell mostly within 10 % while temperature differences were all within 1.2 °C except for N2 mentioned above. Lower temperature recorded at CWA stations could be attributed to monitoring conducted on grassland. Higher WS at CWA stations could be due to the absence of nearby structures, as required by strict installation guidelines. In contrast, shielding from neighboring tall buildings can reduce WS at schools although those included in the analysis did not have buildings of seven floors or more within a radius of 50 m.

In view of the inherent disparity between monitoring on grassland and concrete surface, 1 °C was added to the CWA temperature measurements to re-calculate WBGT. The resulting differences in WBGT fell within 2 °C for most schools with only two exceptions (2.2 °C for S2 and 2.6 °C for N4), excluding N2, the mountain station (3.8 °C) (Table 5 under "plus 1°C scenario"). This finding demonstrated the feasibility of using measurements from the nearest CWA station as a near real-time

Table 4
Comparison of temperature (T, °C), RH (%), WS (m/s), SR (watt/m^2), and WBGT (°C) at the 20 stations between two time periods (10 am to noon versus noon to 1:59 pm) using paired-t-tests.

Station	T 10 am - noon	T noon - 1:59 pm	paired-t *p*-value	RH 10 am - noon	RH noon - 1:59 pm	paired-t *p*-value	WS 10 am - noon	WS noon - 1:59 pm	paired-t *p*-value	SR 10 am - noon	SR noon - 1:59 pm	paired-t *p*-value	WBGT 10 am - noon	WBGT noon - 1:59 pm	paired-t *p*-value
N1	31.1	30.9	0.0187	66.8	67.0	0.2548	0.7	1.0	0.0000	529.3	458.9	0.0000	31.7	30.4	0.0000
N2	30.8	31.2	0.0000	63.5	62.6	0.0003	1.2	1.5	0.0000	574.0	564.9	0.2290	30.5	30.1	0.0000
N3	30.3	30.7	0.0000	68.4	67.3	0.0000	2.2	2.6	0.0000	438.2	419.8	0.0082	29.8	29.5	0.0000
N4	31.3	31.7	0.0000	62.2	61.6	0.0003	0.6	0.7	0.0000	501.8	477.6	0.0000	31.8	31.6	0.0029
N5	30.2	30.6	0.0000	66.8	65.6	0.0000	1.2	1.4	0.0000	523.5	447.7	0.0000	30.0	29.4	0.0000
N6	30.9	31.3	0.0000	63.7	63.0	0.0007	0.9	1.1	0.0000	495.4	443.9	0.0000	30.5	29.9	0.0000
N7	30.8	31.0	0.0000	64.8	64.2	0.0023	1.0	1.1	0.0000	550.4	467.9	0.0000	30.8	30.0	0.0000
N8	29.7	30.0	0.0000	69.4	68.7	0.0000	1.8	2.0	0.0000	543.8	542.3	0.7783	29.4	29.3	0.0734
N9	29.8	30.1	0.0000	70.8	70.0	0.0000	2.0	2.3	0.0000	618.3	608.6	0.0332	29.8	29.8	0.0879
N10	29.9	30.1	0.0000	71.3	70.9	0.0327	2.3	2.6	0.0000	611.4	600.4	0.0172	29.9	29.7	0.0000
C1	31.3	31.9	0.0000	63.8	62.9	0.0000	2.1	2.7	0.0000	623.8	606.5	0.0019	30.7	30.4	0.0000
C2	30.7	31.4	0.0000	67.9	65.7	0.0000	0.7	1.0	0.0000	605.6	536.5	0.0000	32.5	31.6	0.0000
S1	31.1	31.8	0.0000	67.9	65.6	0.0000	1.3	1.8	0.0000	639.4	626.2	0.0038	31.8	31.3	0.0000
S2	31.9	32.8	0.0000	67.1	63.7	0.0000	0.5	0.8	0.0000	626.8	595.8	0.0000	33.9	33.2	0.0000
S3	31.3	31.9	0.0000	69.6	67.2	0.0000	1.3	1.8	0.0000	608.4	586.5	0.0000	31.9	31.4	0.0000
S4	31.9	32.1	0.0000	68.4	67.4	0.0000	0.6	0.9	0.0000	596.5	612.6	0.0007	33.2	32.7	0.0000
S5	29.7	29.9	0.0000	75.9	75.2	0.0000	2.2	2.3	0.0001	694.6	673.9	0.0039	30.7	30.6	0.3829
E1	29.1	29.2	0.0004	74.5	74.4	0.2839	1.2	1.4	0.0000	599.5	513.3	0.0000	30.2	29.4	0.0000
E2	29.7	29.7	0.4936	73.3	74.2	0.0000	0.8	0.9	0.0000	613.0	528.1	0.0000	31.9	30.9	0.0000
E3	30.5	30.5	0.5628	72.4	73.2	0.0000	1.0	1.1	0.0000	686.5	612.9	0.0000	32.1	31.5	0.0000
All	30.6	31.0	0.0000	68.6	67.7	0.0000	1.3	1.5	0.0000	588.9	551.9	0.0000	31.3	30.7	0.0000

Table 5
Comparison of WBGT (°C) between actual measurements obtained from HOBO stations in or near the schools (column A) versus those from the nearest CWA station (column D) and from the scenario of temperature plus 1 °C (column F); all differences in columns E & G were significant at $p < 0.0001$ using paired-t-tests. Column (B) is sample size in terms of hours measured; Column (C) is the distance between the nearest CWA station and the respective HOBO monitor in or near the schools (km).

Station	(A) Mean WBGT in school	(B) Sample sizes	(C) Distance between CWA and the school (km)	(D) Mean WBGT from CWA	(E) Mean WBGT of (School-CWA)	(F) Mean WBGT from CWA (plus 1 °C scenario)	(G) Mean WBGT of (School-CWA) (plus 1 °C scenario)
N1	30.9	9729	10.0	28.5	2.4	29.4	1.5
N2	30.5	4359	5.4	25.7	4.7	26.7	3.8
N3	29.8	5155	0.1	28.2	1.6	29.1	0.7
N4	31.5	6451	3.4	28.1	3.5	29.0	2.6
N5	30.0	5288	1.8	27.6	2.4	28.5	1.5
N6	30.5	8073	4.0	27.8	2.7	28.7	1.8
N7	30.4	7895	4.7	28.3	2.2	29.2	1.3
N8	29.5	9703	17.6	28.2	1.3	29.1	0.4
N9	30.0	9920	5.9	28.6	1.5	29.5	0.6
N10	29.9	10,127	32.3	28.7	1.2	29.6	0.3
C1	30.2	10,562	2.9	29.1	1.1	30.1	0.2
C2	32.0	4873	16.0	29.3	2.7	30.2	1.8
S1	30.9	9993	23.0	29.2	1.7	30.2	0.8
S2	32.6	10,343	3.7	29.5	3.1	30.4	2.2
S3	30.7	8705	17.2	29.0	1.7	29.9	0.8
S4	32.1	9831	8.9	29.8	2.3	30.7	1.4
S5	30.5	5959	8.7	28.6	1.9	29.5	1.0
E1	30.1	8933	0.3	29.0	1.1	29.9	0.2
E2	31.2	8557	1.3	28.6	2.7	29.5	1.7
E3	31.5	10,761	0.6	29.5	2.1	30.4	1.1

warning for those schools after a slight adjustment of 1 °C in temperature.

Tables 6 & 7 present the reduction in WBGT with micro-level adaptation strategies under different scenarios for all schools including N1 and S2, which have the top two highest percentage of WBGTmax ≥36 °C. With shading provided for outdoor activities, WBGT decreased by 2.2–4.2, 2.1–4.4, and 2.9–5.8 °C for all schools, N1, and S2, respectively, during various time periods (Table 6), with the greatest reduction in the morning. The most impactful effect is the reduction in the high-ends of WBGT, from 1.1–9.9 %, 1.6–25.8 %, and 3.0–26.1 % ≥ 36 °C for all schools, N1, and S2, respectively, down to nearly 0 % ≥ 34 °C for all of them, indicating notable reduction in heat-health risks. With outdoor classes relocated to a window-opened indoor environment, WBGT levels decreased by 3.7–5.7, 3.7–6.6, and 4.4–7.3 °C for all schools, N1, and S2, respectively, during various time periods, and percentage of WBGT ≥34 °C was down to 0 for all schools, with the greatest reduction in the morning. In addition, with air-conditioning set at 27 °C in the classrooms, WBGT could further decrease by 3.1–4.2, 2.5–4.3, and 4.0–5.9 °C, respectively (Table 7), with the greatest reduction between noon and 1 pm.

With benefits of exercising/playing in school fields taken into consideration, providing shading, which effectively reduces the percentage of WBGT ≥34 °C to 0, would be the preferred adaptation strategy. However, as outdoor WBGT levels may potentially rise even higher in the future climate, relocating physical classes indoors may serve as an necessary alternative. With windows opened, WBGT levels remain below 34 °C, suggesting that island-wide air-conditioning installation may be of less urgency if resources are limited, and greater priority should be given to those hot spots identified earlier.

4. Discussion

The following discussion focuses on children's WBGT exposure and offers recommendations for schools to reduce children's heat-stress exposures.

Table 6
Reduction in WBGT (°C) and percentage of WBGT ≥36 or 34 °C (threshold of the dangerous or alert category, respectively) in outdoor environments under two outdoor adaptation scenarios compared with actual outdoor measurements (base condition).

		Outdoor WBGT levels		Providing shades outdoors		Opening window indoors	
		Base condition[a]		Scenario 1[b]		Scenario 2[c]	
Schools	Time period	Mean ± SD	WBGT % ≥ 36 °C	Mean ΔWBGT ± SD outdoors compared with actual measurements	WBGT % ≥ 34	Mean ΔWBGT ± SD indoors compared with actual measurements	WBGT % ≥ 34 °C
All schools	8 am to noon	30.8 ± 1.2	9.9	−4.2 ± 0.8	0.0014	−5.7 ± 0.9	0.0
	noon to 1 pm	30.8 ± 1.2	6.2	−3.6 ± 0.7	0.011	−5.1 ± 0.7	0.0
	1 pm to 5 pm	28.7 ± 0.9	1.1	−2.2 ± 0.4	0.0011	−3.7 ± 0.4	0.0
	8 am to 5 pm	29.8 ± 1.0	5.2	−3.1 ± 0.6	0.0023	−4.7 ± 0.6	0.0
N1	8 am to noon	31.3 ± 4.8	25.8	−4.4 ± 2.1	0.0	−6.0 ± 2.1	0.0
	noon to 1 pm	30.8 ± 4.2	12.8	−3.6 ± 1.6	0.0	−5.2 ± 1.6	0.0
	1 pm to 5 pm	28.2 ± 3.8	1.6	−2.1 ± 1.3	0.0	−3.7 ± 1.3	0.0
	8 am to 5 pm	29.8 ± 4.5	12.8	−3.2 ± 2.0	0.0	−4.8 ± 2.0	0.0
S2	8 am to noon	33.4 ± 3.1	26.1	−5.8 ± 1.7	0.0	−7.3 ± 1.7	0.0
	noon to 1 pm	33.5 ± 2.6	19.9	−5.0 ± 1.5	0.0	−6.5 ± 1.5	0.0
	1 pm to 5 pm	30.6 ± 3.0	3.0	−2.9 ± 1.5	0.0	−4.4 ± 1.5	0.0
	8 am to 5 pm	32.0 ± 3.3	14.3	−4.3 ± 2.1	0.0	−5.8 ± 2.1	0.0

[a] Outdoor base condition: actual T, RH, WS, and SR measured.
[b] Scenario 1: T, RH, and WS as measured, and SR = 0.
[c] Scenario 2: T as measured - 1.5, RH and WS as measured, SR = 0.

Table 7
Reduction in WBGT (°C) and percentage of WBGT ≥36 or 34 °C (threshold of the dangerous or alert category, respectively) in indoor environments under one indoor adaptation scenario (scenario 3: air conditioning on) compared with indoor environments with open windows (scenario 2).

		Indoor WBGT levels		Air-conditioning on	
		Scenario 2[a]		Scenario 3[b]	
Schools	Time period	Mean ± SD opening windows	WBGT % ≥ 34 °C	Mean ΔWBGT ± SD indoors compared with opening windows	WBGT % ≥ 34 °C
All schools	8 am to noon	25.1 ± 0.5	0.0	−3.1 ± 0.6	0.0
	noon to 1 pm	25.7 ± 0.6	0.0	−4.2 ± 0.9	0.0
	1 pm to 5 pm	25.0 ± 0.6	0.0	−3.1 ± 0.8	0.0
	8 am to 5 pm	25.1 ± 0.5	0.0	−3.2 ± 0.7	0.0
N1	8 am to noon	25.3 ± 3.2	0.0	−3.5 ± 4.1	0.0
	noon to 1 pm	25.7 ± 3.2	0.0	−4.3 ± 4.2	0.0
	1 pm to 5 pm	24.6 ± 3.1	0.0	−2.5 ± 3.9	0.0
	8 am to 5 pm	25.0 ± 3.2	0.0	−3.1 ± 4.1	0.0
S2	8 am to noon	26.0 ± 2.2	0.0	−4.0 ± 2.8	0.0
	noon to 1 pm	27.0 ± 1.8	0.0	−5.9 ± 2.4	0.0
	1 pm to 5 pm	26.2 ± 2.1	0.0	−4.8 ± 2.6	0.0
	8 am to 5 pm	26.2 ± 2.1	0.0	−4.6 ± 2.7	0.0

[a] Scenario 2: T as measured - 1.5, RH and WS as measured, SR = 0.
[b] Scenario 3: T as 27 °C, RH as measured - 15 %, WS = 0.3 m/s, and SR = 0.

4.1. Children's WBGT exposure

This is the first study assessing children's WBGT exposure. The present findings underscore the importance of assessing children's WBGT exposure, particularly considering the high percentage of days with WBGTmax ≥36 °C, which falls within the dangerous category. Specifically, the mean percentages of WBGTmax ≥36 °C ranged from 2.1 % to 48.5 % in these schools during the monitoring period. Notably S2, N1 and N4 exhibited markedly high percentages (48.5 %, 41.9 % and 37.6 %, respectively), indicating significant heat-stress exposure for children in these areas. Previous epidemiological studies had indicated increased risk of heat-related emergencies for children at WBGTmax ≥33 °C in Taiwan which used outdoor WBGTmax measured on the grassland to represent children's exposure to heat. Our methodology of conducting WBGT assessments in schools, closed to children's actual living environments and activities, provides a more targeted and accurate representation of children's potential heat-stress exposure. In view of the high percentage of days with WBGTmax ≥36 °C in Taiwan, proactive strategies have to be formulated to reduce children's heat-stress exposure and associated health risks. While recent epidemiological studies support WBGT as a suitable heat-stress indicator for the general public (Kakamu et al., 2017; Cheng et al., 2019; Lung et al., 2021), there is a notable gap in research focusing on WBGT exposure assessment for the broader population. Moreover, there is no paper focusing on assessing long-term health impacts of repeated heat exposure during childhood. Under climate change, this issue deserves more attention. Further research in these directions is essential for formulating proper adaptation strategies worldwide.

The significant spatial variations in WBGT observed within the same region, particularly among stations in the Taipei basin, emphasize the importance of conducting on-site WBGT monitoring to assess heat-stress levels and provide real-time warnings. Most schools in Taiwan have measurements for temperature and RH% but lack data for WS and SR. Adequate resources have to be allocated to support on-site WBGT monitoring.

The findings indicating high percentages of hourly WBGT ≥36 °C on both school days and during summer breaks highlight the importance of on-site WBGT monitoring in schools as a valuable warning tool. Given Taiwan's open-school policy, which allows community members to utilize school facilities for exercise and activities after school hours and during summer breaks, the monitoring and warnings help ensure all individuals using school grounds to be aware of potential heat-stress risks and take necessary precautions.

The current analysis highlighted schools' latitude as a determinant influencing the distribution of WBGTmax. However, local geographical features, including basin characteristics, proximity to mountains, the path of the Tropic of Cancer, and overall openness of the surroundings all have influence on heat accumulation around schools. These local features sometimes outweigh the latitude in explaining the spatial variations of WBGT.

Identifying hot spots with WBGTmax in the highly dangerous category (≥ 38 °C, purple days), along with increases in the number of purple days in recent years, underscore the escalating heat-stress levels attributed to climate change. S2 and N1 stand out as particularly concerning, with 51 and 37 days, respectively, recording WBGT ≥38 °C in 2020. Immediate actions to reduce children's WBGT exposure in both schools are imperative.

The present results highlight substantial differences of using WBGT and temperature in identifying/evaluating hot spots, monthly trends, and peak hours of these stations. Compared with temperature, WBGT has been reported to exhibit a stronger and more significant association with heat-related emergency and hospital visits (Cheng et al., 2019; Lung et al., 2021). Therefore, a heat-health warning system should adopt WBGT to accurately identify hot spots and peak hours, enabling the general public, including children, to take appropriate self-protection measures at the high-exposure locations and times. Temperature-based warnings serve other purposes, such as alerting potential infrastructure damage like asphalt melting. For public health protection, warnings issued solely based on temperature alone would overlook the actual high heat-stress hot spots and peak hours.

The observation of higher WBGT levels before noon than in the afternoon has important implications for health adaptation strategies such as class scheduling. Currently, most schools in Taiwan schedule outdoor physical education classes in the morning to avoid temperature peaks, without knowing that heat-stress levels outdoors were significantly higher from 10 am to noon than from noon till 2 pm. Efforts should be made to disseminate such knowledge to prevent children from high WBGT exposure and heat-health risks during the critical hours of 10 am to noon.

Significant temporospatial WBGT variations were observed due to the variations of temperature, RH%, WS, and SR which were affected by air masses (i.e. weather systems) and local topography. Typically, these meteorological parameters are more uniformly distributed in the flat surfaces in the continent of the temperate zone (Ahrens and Henson, 2022). For areas near mountains, near water surfaces (e.g. large lakes, oceans), and in the subtropical or tropical regions where physical obstacles affecting the passage of the air masses or strong moisture fluxes from the surfaces modifying the air masses; significant temporospatial

variations of the meteorological parameters are expected. This further emphasizes the necessity of local WBGT assessment as the basis of formulating fine-spatial-scale heat adaptation strategies in most countries.

Currently, CWA has set up more than 400 automatic stations in Taiwan island consisting of 368 townships, in addition to the 25 standard stations with complete sets of meteorological measurements (https://www.cwa.gov.tw/V8/E/W/OBS_County.html?ID=menu). These automatic stations provide temperature, RH%, and WS measurements transmitted back to CWA and shown in the webpages with a lead time of 10–15 min, without SR. Our findings can be used as the scientific base to increase SR monitors in these automatic stations so that each township has at least one SR monitor. The automatic station with the four meteorological parameters can provide a near real-time heat alert for the schools in the respective township. Moreover, since most countries have the aforementioned areas with high spatial variations of meteorological parameters, our findings can also serve as the scientific foundation for policymakers in other countries to set up automatic stations to provide WBGT alerts to near-by schools. With this type of near real-time heat alert systems for school children, more timely responses can be planned and implemented accordingly. This will facilitate these countries reducing heat-health impacts due to climate change and reaching towards SDG3.

In 2020, UNICEF has estimated that approximately 740 million children (1 in 3 globally) lived in countries experiencing 83 or more days per year with temperature exceeding 35 °C (UNICEF, 2022). The estimation is echoed by our finding that children living around S2 experienced approximately 100 days with WBGT ≥36 °C in 2020, positioning Taiwan among countries facing significant heat stress in the world. Additionally, our results were based on monitoring of May to October. Under climate change, high WBGT levels may also occur on days in November to April. Thus, the numbers of days above 36 °C in the whole year would be further increased. UNICEF has also projected that over 2 billion children, virtually every child on earth, would encounter more frequent heatwaves, even if the world achieves a 'low greenhouse gas emission scenario' (UNICEF, 2022). The present results show that temperature and WBGT exhibit similar trends but peak at different times. To enhance the accuracy of estimating heat stress experienced by children, it would be beneficial for UNICEF to employ the methodology in this study for estimating children's WBGT exposure in future reports.

4.2. Recommendations for preventive measures to reduce children's heat-stress exposures

Children's WBGT exposure could be reduced through various strategies. The evaluated macro-scale adaptation strategy involves utilizing measurements from the nearest CWA station as a near real-time heat alert system for the schools. Our results demonstrated that the estimated WBGT derived from measurements at the nearest CWA station, with a 1 °C temperature increase factored into the inputs, can effectively approximate children's WBGT exposure in school fields with only a 2 °C difference for most schools. With this near real-time warning, school principals and teachers can promptly adjust outdoor class scheduling, children can decide whether to play outdoors during breaks or seek shades for self-protection, and the local government can launch responsive programs and provide services targeting hot spots and vulnerable populations. Prompt reactions to timely warnings would significantly reduce WBGT exposure and heat risks.

There is inevitably uncertainty associated with this +1 °C estimation using data from the nearest station, due to factors such as local geography, distance in between, etc. This uncertainty would affect the reliability of this near real-time heat alert system. Nevertheless, such an estimation is presumably better than not know whether high heat spells occurring locally or receiving heat alerts based on monitoring from even farther locations.

Given sufficient resources, providing real-time warning based on more accurate measurements obtained by on-site WBGT monitoring is preferred. This study demonstrates the advantages of a movable and solar-powered weather station in assessing children's heat-stress exposures with a lead time of 10–15 min. Recent advancement in infrastructure, such as 4G transmission and cloud storage, would facilitate data transmission and integration for calculating massive high-resolution and real-time data that can be maintained in a central site, such as CWA, without burdening the school staff. Contrary to typical meteorological monitoring conducted in a natural environment, such as grassland, without human interference, actual WBGT monitoring should be conducted on surfaces, such as concrete, which children come in contact with, in order to accurately assess their actual heat-stress exposure.

Antoniadis et al. (2020) pointed out that children spend almost one-third of their school time in the schoolyard. Implementing a near real-time warning system for schools is the first step in the heat adaptation strategy, providing school principals, teachers, and local governments with a crucial time window to react and protect children from heat-related risks. UNICEF emphasizes that early warning and monitoring are essential components of a multisectoral heat adaptation plan for children to cope with excess heat (UNICEF, 2023). The US Environmental Protection Agency (USEPA) has suggested action items to parents, caregivers, coaches, and school administrators for reducing children's risks of heat hazards, including keeping kids cool and encouraging them to drink enough water (USEPA, 2023). Health Canada provides tips for parents to reduce the risks of babies, children, and teens due to extreme heat and SR (Health Canada, 2022). These action items and tips should be implemented alongside timely heat warnings.

Both outdoor and indoor micro-scale strategies, which can be implemented by school principals, including providing shades outdoors, relocating physical education classes indoors, and providing air-conditioning indoors, have been found to effectively reduce WBGT, making them crucial for reducing heat stress in hot-spot schools. The most impactful reduction, decreasing the percentage of days in the dangerous category to 0, significantly reduces the heat-health impact on children. More weather extremes are expected in the future. With further increase in outdoor WBGT level, providing air-conditioning indoors would contribute to a significant reduction in WBGT. Nevertheless, if brown energy is used, electricity consumption becomes the drawback of this strategy.

In Taiwan, the highest WBGT levels in the diurnal cycle typically occur from 10 am to noon; hence, scheduling outdoor physical education classes during this time period should be avoided. Moreover, exercise would generate internal body heat; therefore, it is advisable to lower the intensity of physical activities during high WBGT periods. Furthermore, special attention should be given to physically challenged children and susceptible students with pre-existing medical conditions because they are particularly vulnerable among school-aged children.

There are challenges in implementing these macro-scale or micro-scale strategies, especially for resource-limited areas. It requires resource, manpower, and expertise to setup and maintain a near real-time heat alert system in a school even with a station using a solar panel. Thus, receiving warnings from an existing agency would be an easier choice which needs support and consensus of the policymakers in central or city levels, that in turn is a challenge as well. For micro-scale strategies, providing shades outdoors and air conditioning indoors also need funding support for installation and subsequent maintenance. Thus, reschedule outdoor activities according to alerts is the most inexpensive choice. Either way, enhancing awareness of the school principals, teachers, and students is crucial in implementing any adaptation strategies. Education and communication among different levels from the authorities to the recipients on the potential impacts of heat stress and the proper responsive actions to protect themselves are sometimes challenging. Nevertheless, we must overcome these obstacles in order to reduce heat health risks of children.

This study has several limitations. First, to avoid disrupting students'

activities, our monitors were predominantly placed at heights of 12–20 m. Consequently, WS measurements were higher than those measured at ground level, where wind flow may be blocked by trees or buildings. In other words, the WBGT measurements may underestimate the actual heat stress children experienced. Even with such underestimates, significant percentages of WBGT $\geq$36 °C were found, demonstrating high heat stress experienced by children in schools. Secondly, the less expensive anemometer used with a resolution of 0.5 m/s is not as accurate as the CWA monitors. Nevertheless, it can still estimate what children experienced with the advantage of cost-saving. Thirdly, there are uncertainty in the representativeness of these measurements to the actual heat exposures of those children due to aforementioned or other factors such as distance. Nevertheless, these monitors were mostly within 500 m from the center of the school fields children play outdoors, such an estimation shall provide more close-to-reality exposure estimates than obtaining exposure from even farther stations. Fourthly, 19 HOBO monitors were set on concrete surfaces and one on grassland. As observed, children also spent time on other surfaces such as asphalt and synthetic-rubber (polyurethane) running tracks in schools. For safety reasons, we were not able to place monitors on those surfaces in this seven-year monitoring. Thus, our results do not cover WBGT experienced on those surfaces. Finally, the findings in the relationships of WBGT in schools and nearby CWA stations can only be generalized to schools with similar construction materials and geographic conditions such as those in flat surfaces, not to schools in or near mountains. Nevertheless, the findings in evaluating the micro-scale strategies shall be able to be generalized to other schools in Taiwan since the building materials and window design are similar.

This pioneering assessment on children's WBGT exposure using measurements from a real-time monitoring network in or near schools reveals prevalence of high WBGT levels in the dangerous or highly dangerous category, particularly in the hot-spot schools with more than 30 % of days with WBGTmax $\geq$36 °C every year. The observation that WBGT levels exhibit different hot spots and peak hours compared with temperature underscores the importance of incorporating WBGT into the heat-health warning system for effective public health protection.

To accurately estimate WBGT exposure for children as a real-time warning tool, on-site WBGT monitoring should be set up in each school or measurements at the nearest CWA should be taken with temperature plus 1 °C adjustment. To reduce heat exposure when outdoor WBGT exceeds 36 °C, shades should be provided outdoors or outdoor physical education classes should be relocated indoors. Air-conditioning can be provided indoors to further reduce heat-stress. Scheduling outdoor physical classes according to local peak hours of WBGT to avoid excessive heat exposure is highly advised. To obtain actual heat-stress levels, monitoring WBGT on surfaces children mostly encounter is recommended.

Future research may explore whether other adaptation strategies, such as greenness in or around the schools, would reduce children's WBGT levels. Scientists and policy makers may also consider to set up such a WBGT monitoring network to evaluate the temporospatial WBGT variations and the percentage of health-concerned WBGT levels in their countries as the foundation of formulating heat adaptation strategies. The lessons learned and the methodology employed in this study offer useful references for scientists and policymakers worldwide in monitoring WBGT for children and implementing effective measures to reduce children's heat stress levels. Given that this is currently an understudied topic, the present findings can serve as a foundation for future research and policy development aimed at protecting children from adverse effects of heat stress.

CRediT authorship contribution statement

Shih-Chun Candice Lung: Writing – review & editing, Writing – original draft, Supervision, Resources, Project administration, Methodology, Funding acquisition, Conceptualization. **Shu-Chuan Hu:** Writing – review & editing, Writing – original draft, Visualization, Software, Project administration, Formal analysis, Data curation, Conceptualization. **Chun Hu Liu:** Writing – review & editing, Visualization, Software, Formal analysis. **Tzu-Yao Julia Wen:** Writing – review & editing, Project administration, Investigation. **Wen-Cheng Vincent Wang:** Writing – review & editing, Investigation.

Declaration of competing interest

The authors declare that they have no known competing financial interests or personal relationships that could have appeared to influence the work reported in this paper.

Acknowledgement

We would like to acknowledge the funding support from the Academia Sinica thematic project “Integrated Multi-source and High-resolution Heat Wave Vulnerability Assessment of Taiwan (AS-104-SS-A02)” and “Trans-disciplinary $PM_{2.5}$ Exposure Research in Urban Areas for Health-oriented Preventive Strategies (AS-107-SS-A03)” of Academia Sinica, Taiwan, as well as Project Nos. 107-2621-M-001-003 and 108-2621-M-001-004 of the National Science and Technology Council, Executive Yuan, Taiwan. We also appreciate the support of all the schools and institutions in establishing and maintaining the monitoring network. The contents of this paper are solely the responsibility of the authors and do not represent the official views of the aforementioned institutes and funding agencies.

Appendix A. Supplementary data

Supplementary data to this article can be found online at https://doi.org/10.1016/j.scitotenv.2024.176840.

Data availability

We provide links to data repositories in the “Methods” section.

References

Ahrens, D.C., Henson, R., 2022. Meteorology Today: An Introduction to Weather, Climate and the Environment, 12th ed. Cengage Learning.

Antoniadis, D., Katsoulas, N., Papanastasiou, D.K., 2020. Thermal environment of urban schoolyards: current and future design with respect to Children's thermal comfort. Atmosphere 11 (11), 1144. https://doi.org/10.3390/atmos11111144.

Bernard TE. Thermal stress. In Fundamentals of Industrial Hygiene, 6th ed.; Plog, B.A., Quinlan, P., Eds.; National Safety Council: Itasca, IL, USA, 2012; Chapter 12, pp. 335–361.

Bröde, P., Fiala, D., Lemke, B., Kjellstrom, T., 2018. Estimated work ability in warm outdoor environments depends on the chosen heat stress assessment metric. Int. J. Biometeorol. 62 (3), 331–345. https://doi.org/10.1007/s00484-017-1346-9.

Central Weather Administration (CWA), 2022. https://www.cwa.gov.tw/V8/C/K/Encyclopedia/climate/climate2_list.html.

Cheng, Y.T., Lung, S.C.C., Hwang, J.S., 2019. New approach to identifying proper thresholds for a heat warning system using health risk increments. Environ. Res. 170, 282–292. https://doi.org/10.1016/j.envres.2018.12.059.

Chou, C.C.K., Lung, S.-C.C., Hsiao, T.-C., Lee, C.-T., 2023. Regional and urban air quality in East Asia: Taiwan. In: In. Springer Nature Singapore, pp. 469–506. https://doi.org/10.1007/978-981-15-2760-9_71.

Coccolo, S., Kämpf, J., Scartezzini, J.-L., Pearlmutter, D., 2016. Outdoor human comfort and thermal stress: a comprehensive review on models and standards. Urban Clim. https://doi.org/10.1016/j.uclim.2016.08.004.

Copernicus Climate Change Service (C3S). 2023. “2023 June–July-August Season highlights”. C3S, European Commission. https://climate.copernicus.eu/summer-2023-hottest-record.

Falk, B., Dotan, R., 2008. Children's thermoregulation during exercise in the heat - a revisit. Applied Physiology Nutrition and Metabolism-Physiologie Appliquee Nutrition Et Metabolisme. 33 (2), 420–427. https://doi.org/10.1139/h07-185.

Health Canada, 2022. Sun Safety tips for parents. Health Canada. www.canada.ca/en/health-canada/services/sun-safety/sun-safety-tips-parents.html.

Hodges, G.J., Kiviniemi, A.M., Mallette, M.M., Klentrou, P., Falk, B., Cheung, S.S., 2018. Effect of passive heat exposure on cardiac autonomic function in healthy children. Eur. J. Appl. Physiol. 118 (10), 2233–2240. https://doi.org/10.1007/s00421-018-3957-1.

Höppe, P. 2002. Different aspects of assessing indoor and outdoor thermal comfort [Article; Proceedings Paper]. Energy and Buildings, 34(6), 661-665, Article Pii s0378-7788(02)00017-8. doi:https://doi.org/10.1016/s0378-7788(02)00017-8.

International Standards Organization (ISO). 2017. Ergonomics of the Thermal Environment — Assessment of Heat Stress Using the WBGT (Wet Bulb Globe Temperature) Index. https://www.iso.org/standard/67188.html.

IPCC, 2021: Climate Change 2021: The Physical Science Basis. Contribution of Working Group I to the Sixth Assessment Report of the Intergovernmental Panel on Climate Change [Masson-Delmotte, V., P. Zhai, A. Pirani, S.L. Connors, C. Péan, S. Berger, N. Caud, Y. Chen, L. Goldfarb, M.I. Gomis, *M. Huang*, K. Leitzell, E. Lonnoy, J.B.R. Matthews, T.K. Maycock, T. Waterfield, O. Yelekçi, R. Yu, and B. Zhou (eds.)]. Cambridge University Press, Cambridge, United Kingdom and New York, NY, USA, In press, doi:https://doi.org/10.1017/9781009157896.

IPCC, 2022: Climate Change 2022: Impacts, Adaptation, and Vulnerability. Contribution of Working Group II to the Sixth Assessment Report of the Intergovernmental Panel on Climate Change [H.-O. Pörtner, D.C. Roberts, M. Tignor, E.S. Poloczanska, K. Mintenbeck, A. Alegría, M. Craig, S. Langsdorf, S. Löschke, V. Möller, A. Okem, B. Rama (eds.)]. Cambridge University Press. Cambridge University Press, Cambridge, UK and New York, NY, USA, 3056 pp., doi:https://doi.org/10.1017/9781009325844.

ISO 7243, Hot environments — Estimation of the heat stress on working man, based on the WBGT-index (wet bulb globe temperature). 1989. https:/standards.iteh.ai/catalog/standards/sist/771d79c0-d0fd-4875-b085ac605c6557bc/iso-7243-1989.

Kakamu, T., Wada, K., Smith, D.R., Endo, S., Fukushima, T., 2017. Preventing heat illness in the anticipated hot climate of the Tokyo 2020 summer Olympic games. Environ Health Prev. 22 (1). https://doi.org/10.1186/s12199-017-0675-y.

Lemke, B., Kjellstrom, T., 2012. Calculating workplace WBGT from meteorological data: a tool for climate change assessment. Ind. Health 50 (4), 267–278. https://doi.org/10.2486/indhealth.ms1352.

Liljegren, J.C., Carhart, R.A., Lawday, P., Tschopp, S., Sharp, R., 2008. Modeling the wet bulb globe temperature using standard meteorological measurements. J. Occup. Environ. Hyg. 5 (10), 645–655. https://doi.org/10.1080/15459620802310770.

Lin, Y.K., Chang, C.K., Li, M.H., Wu, Y.C., Wang, Y.C., 2012. High-temperature indices associated with mortality and outpatient visits: characterizing the association with elevated temperature. Sci. Total Environ. 427, 41–49. https://doi.org/10.1016/j.scitotenv.2012.04.039.

Lung, S.C.C., Yeh, J.C.J., Hwang, J.S., 2021. Selecting thresholds of heat-warning systems with substantial enhancement of essential population health outcomes for facilitating implementation. IJERPH 18 (18), 9506. https://doi.org/10.3390/ijerph18189506.

Lung, S.C.C., Liou, M.-L., Yeh, J.-C.J., Hwang, J.-S., 2023. A pilot heat-health warning system co-designed for a subtropical city. PloS One 18 (11), e0294281. https://doi.org/10.1371/journal.pone.0294281.

National Aeronautics and Space Administration (NASA). 2022 A July of Extremes - NASA Earth Observatory. https://earthobservatory.nasa.gov/images/150152/a-july-of-extremes.

Occupational Safety and Health Administration (OSHA), 2017. Chapter 4 heat stress. OSHA Technical Manual (OTM) Section III, updated (September 15, 2017). https://www.osha.gov/otm/section-3-health-hazards/chapter-4#introduction.

Santana, J.R.R., Riverabrown, A.M., Frontera, W.R., Rivera, M.A., Mayol, P.M., Baror, O., 1995. Effect of drink pattern and solar-radiation on thermoregulation and fluid balance during exercise in chronically heat acclimatized children. Am. J. Hum. Biol. 7 (5), 643–650. https://doi.org/10.1002/ajhb.1310070512.

Sheffield, P.E., Landrigan, P.J., 2011. Global climate change and children's health: threats and strategies for prevention. Environ Health Persp. 119 (3), 291–298. https://doi.org/10.1289/ehp.1002233.

Spector, J.T., Sheffield, P.E., 2014. Re-evaluating occupational heat stress in a changing climate. Ann. Occup. Hyg. 58 (8), 936–942. https://doi.org/10.1093/annhyg/meu073.

Taiwan National Development Council, 2018. Government website open information announcement. https://data.gov.tw/en.

The Lancet Planetary, H, 2022. Be prepared for more heat. The Lancet Planetary Health. 6 (9), e706. https://doi.org/10.1016/s2542-5196(22)00201-7.

Tsuzuki, K. 2023. Effects of heat exposure on the thermoregulatory responses of young children. J. Therm. Biol. 113:8. Article 103507. doi:https://doi.org/10.1016/j.jtherbio.2023.103507.

Uibel, D., Sharma, R., Piontkowski, D., Sheffield, P.E., Clougherty, J.E., 2022. Association of ambient extreme heat with pediatric morbidity: a scoping review. Int. J. Biometeorol. 66 (8), 1683–1698. https://doi.org/10.1007/s00484-022-02310-5.

United Nations (UN). Sustainable Development Goals (SDGs). 2018. Available online: https://www.un.org/sustainabledevelopment/. (accessed on 26 January 2021).

United Nations Children's Fund (UNICEF), 2022. The Coldest Year of the Rest of their Lives: Protecting Children from the Escalating Impacts of Heatwaves. UNICEF, New York.

United Nations Children's Fund (UNICEF), 2023. Protecting Children from Heat-Stress-a Technical Note. UNICEF, Health Programme, Programme Group, New York, NY 10017, USA.

United Stations Environmental Protection Agency (USEPA), 2023. Climate Change and Children's Health; USEPA, https://www.epa.gov/climateimpacts/climate-change-and-childrens-health.

Vanos, J.K., 2015. Children's health and vulnerability in outdoor microclimates: a comprehensive review. Environ. Int. 76, 1–15. https://doi.org/10.1016/j.envint.2014.11.016.

World Health Organization (WHO), 2022, "Heatwave in Europe: local resilience saves lives – global collaboration will save humanity", WHO news, https://www.who.int/europe/news/item/22-07-2022-heatwave-in-europe–local-resilience-saves-lives—global-collaboration-will-save-humanity.

Wu, C.D., Lung, S.C.C., 2016. Application of 3-D urbanization index to assess impact of urbanization on air temperature. Sci. Rep. 6. Article 24351. https://doi.org/10.1038/srep24351.

Yaglou, C.P., Minard, D., 1957. Control of heat casualties at military training centers. A. M.a. archives of. Ind. Health 16 (4), 302–316. https://doi.org/10.21236/AD0099920.